Cell Stem Cell
Article

Directed Differentiation and Functional Maturation of Cortical Interneurons from Human Embryonic Stem Cells

Asif M. Maroof,[1,2,8] Sotirios Keros,[4,5] Jennifer A. Tyson,[3] Shui-Wang Ying,[4] Yosif M. Ganat,[1,2] Florian T. Merkle,[8] Becky Liu,[1,2] Adam Goulburn,[3] Edouard G. Stanley,[6,10] Andrew G. Elefanty,[6,10] Hans Ruedi Widmer,[7] Kevin Eggan,[8] Peter A. Goldstein,[4] Stewart A. Anderson,[3,9,*] and Lorenz Studer[1,2,*]
[1]Center for Stem Cell Biology
[2]Developmental Biology Program
Sloan-Kettering Institute for Cancer Research, 1275 York Ave, New York, NY 10065, USA
[3]Department of Psychiatry
[4]Department of Anesthesiology
[5]Division of Pediatric Neurology, Department of Pediatrics
Weill Cornell Medical College, 1300 York Ave, New York, NY 10021, USA
[6]Monash Immunology and Stem Cell Laboratories, Monash University, Building 75, STRIP1, West Ring Road, Clayton, Victoria 3800, Australia
[7]Department of Neurosurgery, University of Bern, Inselspital, CH-3010 Bern, Switzerland
[8]Department of Stem Cell and Regenerative Biology, Harvard University, Cambridge, MA 02138, USA
[9]Department of Psychiatry, Children's Hospital of Philadelphia and University of Pennsylvania Medical School, Philadelphia, PA 19104, USA
[10]Murdoch Childrens Research Institute, The Royal Children's Hospital, Flemington Road, Parkville, Victoria 3052, Australia
*Correspondence: andersons3@email.chop.edu (S.A.A.), studerl@mskcc.org (L.S.)
http://dx.doi.org/10.1016/j.stem.2013.04.008

SUMMARY

Human pluripotent stem cells are a powerful tool for modeling brain development and disease. The human cortex is composed of two major neuronal populations: projection neurons and local interneurons. Cortical interneurons comprise a diverse class of cell types expressing the neurotransmitter GABA. Dysfunction of cortical interneurons has been implicated in neuropsychiatric diseases, including schizophrenia, autism, and epilepsy. Here, we demonstrate the highly efficient derivation of human cortical interneurons in an *NKX2.1::GFP* human embryonic stem cell reporter line. Manipulating the timing of SHH activation yields three distinct GFP+ populations with specific transcriptional profiles, neurotransmitter phenotypes, and migratory behaviors. Further differentiation in a murine cortical environment yields parvalbumin- and somatostatin-expressing neurons that exhibit synaptic inputs and electrophysiological properties of cortical interneurons. Our study defines the signals sufficient for modeling human ventral forebrain development in vitro and lays the foundation for studying cortical interneuron involvement in human disease pathology.

INTRODUCTION

Human pluripotent stem cells (hPSCs) are a powerful tool for the study of human development and disease and for applications in regenerative medicine. The use of hPSCs differentiated toward CNS lineages has been of particular interest given the lack of effective therapies for many neurodegenerative and neuropsychiatric disorders and the availability of protocols for efficiently directing neuronal specification in vitro (Chambers et al., 2009). Early studies using hPSCs have been primarily geared toward neurodegenerative disorders, which are known to affect specific neuron types such as midbrain dopamine neurons in Parkinson's disease (PD; Kriks et al., 2011) or motor neurons in amyotrophic lateral sclerosis (ALS; Dimos et al., 2008) and spinal muscular atrophy (SMA; Ebert et al., 2009). More recent studies suggest the possibility of tackling complex neuronal disorders such as schizophrenia (Brennand et al., 2011) or autism-related syndromes (Marchetto et al., 2010; Paşca et al., 2011). Unlike in PD, ALS, and SMA, the neuron types critical for modeling schizophrenia or autism are less well defined, and no attempts have been made to direct neuron subtype identity in those studies. There has been considerable progress in establishing protocols for the derivation of human embryonic stem cell (ESC)-derived cortical projection neurons (Espuny-Camacho et al., 2013; Shi et al., 2012). However, inhibitory neurons such as cortical interneurons may be particularly important in schizophrenia or autism (Insel, 2010; Lewis et al., 2005). We have previously demonstrated the derivation of cortical interneurons using an *Lhx6::GFP* reporter mouse ESC line (Maroof et al., 2010). However, the efficiency of cortical interneuron generation was low, and it was uncertain whether those conditions would apply for generating human cortical interneurons from PSCs. Modeling the development of human cortical interneurons in vitro is of particular interest, because their developmental origin is controversial: studies suggest considerable differences across mammalian species (Letinic et al., 2002; Yu and Zecevic, 2011). Furthermore, the protracted in vivo development of several cortical interneuron types (Anderson et al., 1995) represents an additional challenge for modeling their differentiation using human cells in vitro.

Here, we present a small-molecule-based strategy for the efficient induction of human cortical interneurons. Exposure to the tankyrase inhibitor XAV939 enhances forebrain differentiation. Using an *NKX2.1::GFP* hESC reporter line, we demonstrate the selective derivation of three distinct ventral forebrain precursor populations by combining XAV939 treatment with the timed activation of sonic hedgehog (SHH) signaling. Importantly, results in both hPSCs and human embryos reveal differences between mouse and human forebrain development, such as the human-specific, yet transient, FOXA2 expression within the ventral forebrain. Finally, mature functional properties and the expression of late cortical interneuron markers, including parvalbumin (PV) and somatostatin (SST), demonstrate the feasibility of studying human cortical interneuron differentiation from hPSCs in vitro despite their protracted development in vivo.

RESULTS

Combined Inhibition of Wnt and Activation of SHH Signaling Triggers Efficient Induction of NKX2.1+ Neural Precursors

The first step in modeling cortical interneuron development is the robust induction of forebrain precursors. Specification of anterior and forebrain fate is considered a default program during neural differentiation of hPSCs (Chambers et al., 2009; Eiraku et al., 2008; Espuny-Camacho et al., 2013; Gaspard et al., 2008). However, not all cell lines adopt anterior neural fates at equal efficiencies (Kim et al., 2011; Wu et al., 2007). Patterning factors secreted within differentiating cultures such as fibroblast growth factors (FGFs), Wnts, or retinoids can suppress forebrain induction and trigger the induction of caudal cell fates. We recently reported that early, high-dose SHH treatment also suppresses forebrain markers such as FOXG1 via inhibition of DKK1 induction (Fasano et al., 2010). This is a concern for deriving cortical interneurons that are thought to require strong SHH activation at the NKX2.1+ progenitor stage (Xu et al., 2010). Here, we tested whether pharmacological inhibition of WNT signaling can improve FOXG1 induction and subsequently enable the controlled, SHH-mediated ventralization toward NKX2.1+ forebrain progenitor fates (Figure 1A).

Neural differentiation of hESCs via the dual SMAD-inhibition protocol (Chambers et al., 2009) using Noggin + SB431542 (NSB) robustly induced FOXG1+/PAX6+ precursors. Replacement of Noggin with the ALK2/ALK3 inhibitor LDN-193189 (LSB) induced PAX6 expression equally well but showed a trend toward lower percentages of FOXG1+ cells (Figures 1B and 1C). Adding recombinant DKK1 or the tankyrase inhibitor XAV939 (Huang et al., 2009), inhibitors of canonical Wnt signaling, enhanced FOXG1 expression in LSB-treated cultures (Figures 1B–1D). Importantly, the effect of XAV939 on FOXG1 induction was consistent (Figure 1E) across multiple independent hESC (HES-3 and WA-09) and human induced PSC (iPSC) lines (C72 line, Papapetrou et al., 2009; SeV6, Kriks et al., 2011). Therefore, the use of three small molecules (XAV939, LSB, and SB431542; termed XLSB) enables rapid and robust induction of forebrain fates across human ESCs and iPSC lines.

We next wanted to test our ability to induce ventral fates using XLSB in the presence of SHH activators (Figure 1A). The transcription factor NKX2.1 is a marker of ventral prosencephalic progenitor populations (Sussel et al., 1999; Xu et al., 2004). Using a previously established *NKX2.1::GFP* knockin reporter hESC line (Goulburn et al., 2011), we observed GFP induction by day 10 following activation of the SHH pathway by recombinant SHH (R&D Systems, C-25II) and the smoothened activator purmorphamine (Figure 1F). We found maximal induction of *NKX2.1::GFP* at day 18 upon treatment with 1 μM purmorphamine and 5nM SHH (Figure 1G), a condition referred to as "SHH" for the remainder of the manuscript. Our past studies on the derivation of hESC-derived floor plate cells demonstrated that early treatment with SHH (day 1 of differentiation) is critical for the efficient induction of FOXA2 (Fasano et al., 2010). In contrast, we observed here that cells exposed to SHH at late differentiation stages (day 10 of the XLSB protocol) remain competent for inducing *NKX2.1::GFP* as measured by fluorescence-activated cell sorting (FACS) (Figure 1H). Therefore, XLSB+SHH treatment represents a strategy for generating NKX2.1+ progenitors at high efficiencies.

Timing of SHH Exposure Induces Distinct Ventral Progenitor Populations

The efficient induction of NKX2.1 largely independent of the timing of SHH exposure raised the question of whether timing impacts the subtype of NKX2.1+ neural progenitors generated. Analogous to rodents, NKX2.1 is expressed during early neural human development in both the FOXG1+ telencephalon and the FOXG1-negative ventral diencephalon (Figure 2A; Kerwin et al., 2010; Rakic and Zecevic, 2003). During embryonic mouse development, NKX2.1 expression in the telencephalon (FOXG1+) is restricted to the ventral (subcortical) domain. In contrast, reports in human fetal tissue suggested that NKX2.1 may not be restricted to the ventral forebrain, instead extending into the dorsal forebrain and cortical anlage (Rakic and Zecevic, 2003; Yu and Zecevic, 2011). However, those studies were largely based on the analysis of second-trimester human fetuses, making it difficult to distinguish whether NKX2.1+ cells were induced in the dorsal forebrain or migrated dorsally after induction in the ventral domain (Fertuzinhos et al., 2009). By performing immunocytochemical analyses in early-stage human embryos (Carnegie stage 15 [CS15], ~38 days post conception), we observed restriction of NKX2.1 expression to the ventral forebrain (Figures 2B–2E) comparable to the developing mouse CNS. The NKX2.1 domain in the human embryonic ventral forebrain was further subdivided into an OLIG2+ ganglionic eminence and an OLIG2-negative preoptic-area anlage (Figures 2C and 2D).

To address whether in vitro timing of SHH exposure affects the regional identity of the resulting hPSC-derived *NKX2.1::GFP*+ cells, we compared the identities of sorted cells at day 18 of differentiation (Figure 2F). In agreement with our previous results on floor-plate induction (Fasano et al., 2010), we observed that early SHH exposure (days 2–18) suppressed FOXG1 induction (Figure 2G, left panel) despite robust induction of *NKX2.1::GFP* (see Figure 1H). In contrast, both day 6–18 and day 10–18 treatment groups showed expression of FOXG1 but differed in OLIG2 expression (Figure 2G, middle and right panels). We hypothesize that differential expression of FOXG1 and OLIG2 reflect the distinct NKX2.1+ precursor domains observed during early human development (Figures 2A–2E) and mimic the Olig2+ domains during mouse forebrain development (Flames

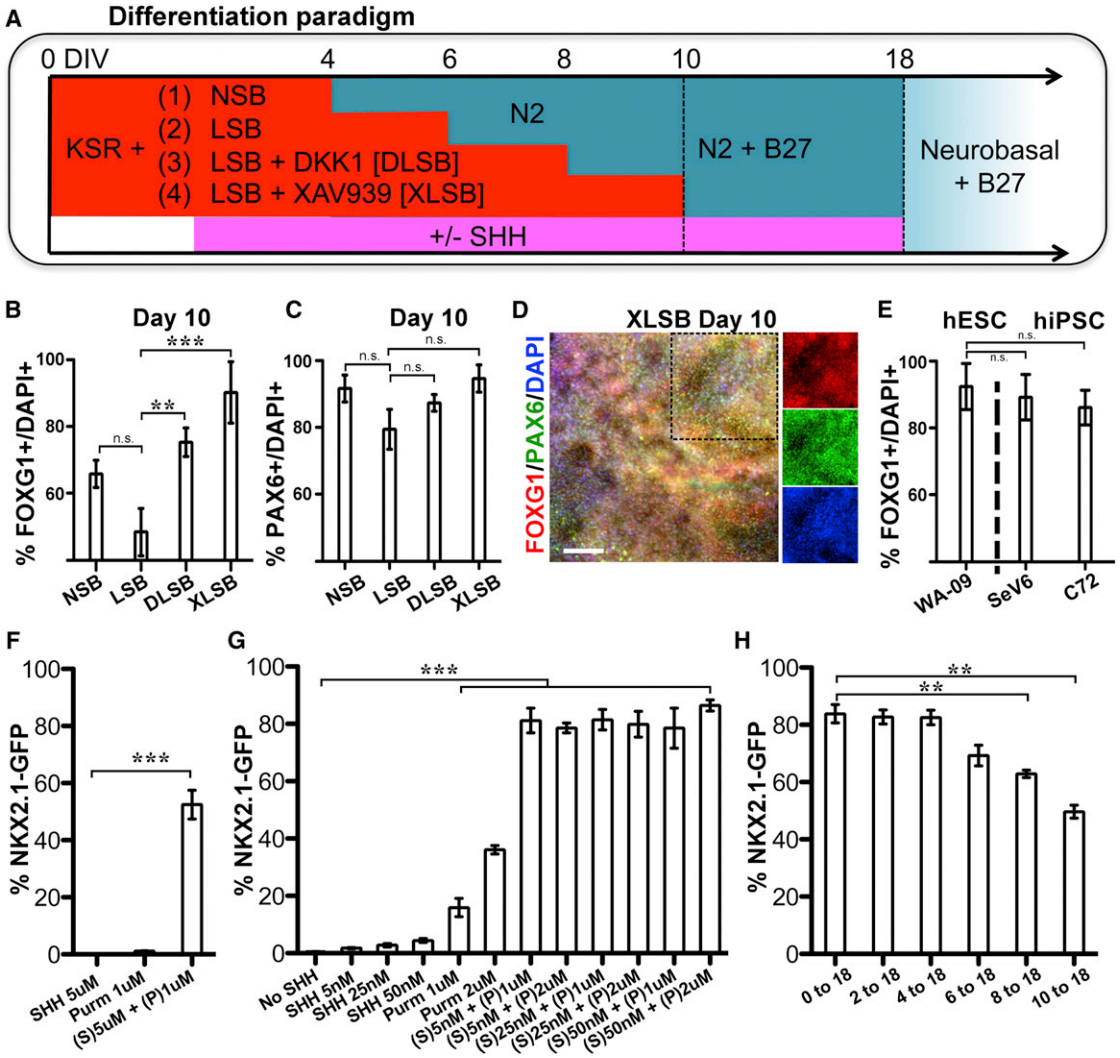

Figure 1. Wnt Inhibition and Activation of SHH Signaling Yields Highly Efficient Derivation of Forebrain Fates and NKX2.1 Induction

(A) Schematic of the differentiation protocol in the dual-SMAD inhibition paradigm for generating anterior neural progenitors.

(B–E) When either DKK1 or XAV939, both Wnt-signaling antagonists, was added to the dual-SMAD inhibition protocol (DLSB or XLSB), there was a significant increase in the percentage of FOXG1+ cells (B) without a loss of PAX6 expression (C): $^{**}p < 0.01$; $^{***}p < 0.001$; n.s., not significant; using ANOVA followed by Scheffe test. (D) Representative immunofluorescent image for FOXG1 (red) and PAX6 (green) expression at day 10 following XLSB treatment. Single-channel fluorescent images of the marked region are shown in the three right panels. (E) Robust telencephalic specification using XLSB was also observed at comparable efficiencies in hiPSCs (lines SeV6 and C72; n = 4).

(F–H) Addition of SHH signaling to the XLSB protocol significantly enhanced the production of *NKX2.1::GFP*-expressing progenitors. (F) Added from day 4, 5 nM SHH (C24II) and 1 μm purmorphamine showed synergistic effects in inducing *NKX2.1::GFP* expression at day 10 ($^{***}p < 0.001$, compared to SHH). A range of concentrations of SHH and purmorphamine are compared at day 18 in (G), and again, cotreatment was greatly superior to quite high concentrations of either SHH or purmorphamine alone ($^{***}p < 0.001$, compared to no SHH, using ANOVA followed by Scheffe test). (H) Delaying the timing of SHH exposure between 2 and 10 days of differentiation did not dramatically affect the efficiency of *NKX2.1::GFP* induction measured at day 18 ($^{***}p < 0.001$ compared to 0–18, using ANOVA followed by Scheffe test). P, purmorphamine; S, sonic hedgehog.

Data are from hESC line HES-3 (*NKX2.1::GFP*) in (B), (C), and (F)–(H); from hESC line WA-09/H9 in (D); and from hESC line WA-09/H9 and hiPSC lines SeV6 and C72 in (E). The scale bar in (D) represents 125 μm. Data in (B), (C), and (E)–(H) are represented as the mean ± SEM.

et al., 2007). More than 90% of the *NKX2.1::GFP*+ cells in the 6–18 and 10–18 protocols coexpressed FOXG1, and nearly 80% of the GFP+ cells in the 10–18 protocol coexpressed OLIG2 (Figure 2H).

The impact of the timing of SHH exposure on the derivation of specific ventral precursor populations was further examined by global transcriptome analysis (Figures 2I–2K; Table S1 available online; all raw data are available in the Gene Expression Omnibus [GEO], http://www.ncbi.nlm.nih.gov/geo/). A direct comparison of day 10–18 versus untreated cultures (no SHH) confirmed the robust induction of ventral specification markers such as *NKX2.1*, *NKX2.2*, *ASCL1*, *SIX6*, *OLIG2*, and *NKX6.2*, which were induced at the expense of dorsal forebrain markers such as *EMX2* and *PAX6* (Figure 2I). There were no significant

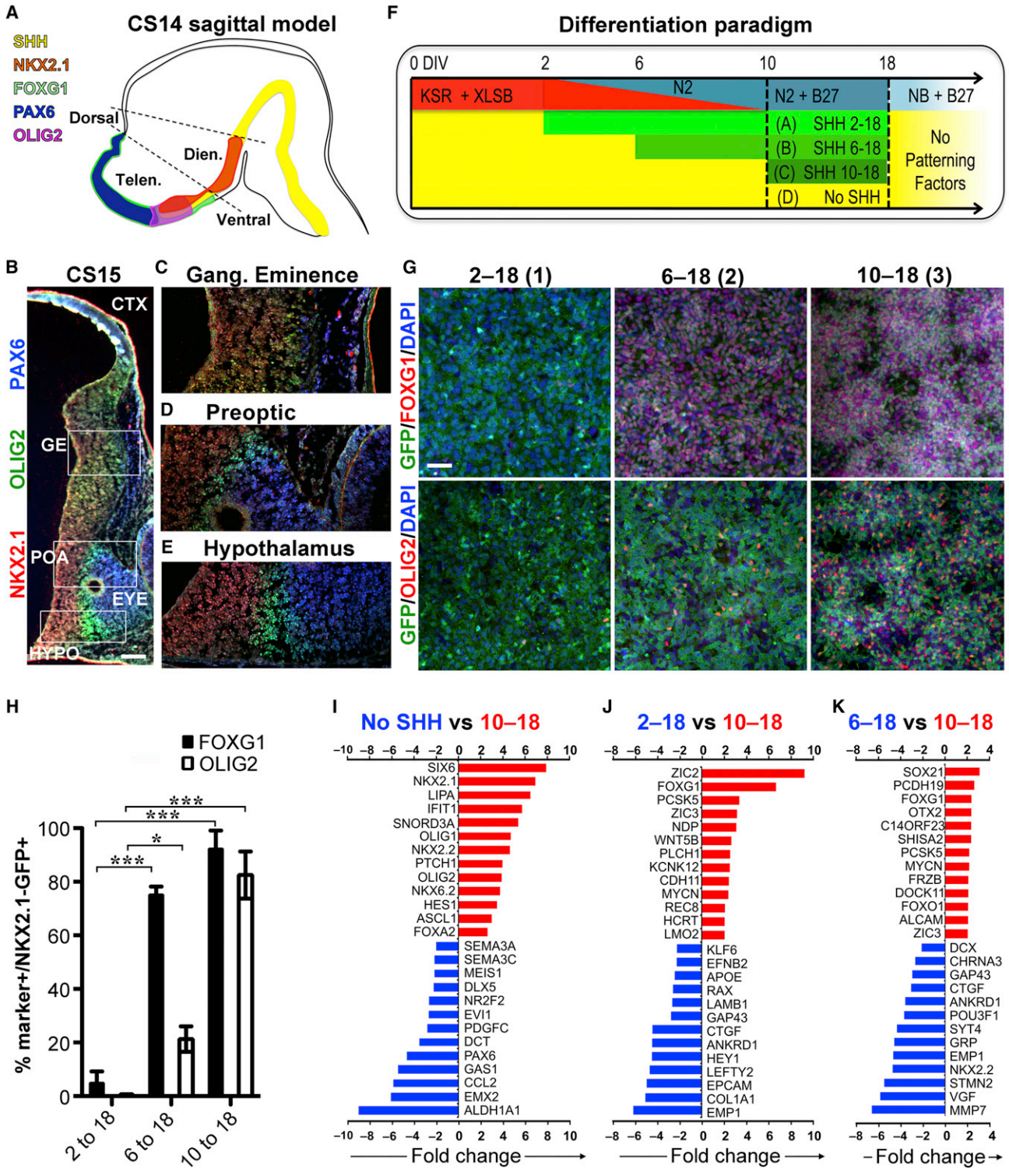

Figure 2. Timing of SHH Exposure Determines the Regional Identity of *NKX2.1::GFP*-Expressing Progenitors

(A) Model of human prosencephalon (sagittal view at CS14) with expression of forebrain patterning markers based on published data (Kerwin et al., 2010). Dien., diencephalon; Tien., telencephalon.

(B–E) Coronal (oblique) hemisection of the human prosencephalon at CS15 demonstrates expression of NKX2.1, OLIG2, and PAX6. NKX2.1 and OLIG2 are expressed in various regions throughout the ventral prosencephalon, whereas PAX6 is restricted to the dorsal prosencephalon and the eye. CTX, cortex; POA, preoptic area; HYPO, hypothalamus. The scale bar in (B) represents 200 μm. The expression of these proteins is nonoverlapping, except in the ganglionic eminence (GE) (C), where OLIG2 and NKX2.1 are coexpressed.

(legend continued on next page)

differences in the expression of general anterior markers such as *FOXG1* and *OTX2* (Figure 2I), supporting the notion that both populations are of a forebrain identity. Comparison of day 10–18 and day 2–18 treated cultures (Figure 2J) illustrated differences in the expression of anterior markers such as *FOXG1* versus diencephalic markers such as *RAX*. In contrast, day 10–18 versus day 6–18 treated cultures showed less pronounced differences in forebrain marker expression (Figure 2K). Overall, our data demonstrate that the window of SHH treatment significantly impacts the identity of hPSC-derived NKX2.1 precursors.

One surprising finding from the gene-expression data was the induction of FOXA2 in all SHH-treated cultures (Figure 2I). Expression of FOXA2, a marker thought to be largely restricted to the floor plate within the developing CNS, was confirmed at day 18 of differentiation in *NKX2.1::GFP*+ cells of all three SHH treatment paradigms (Figures S1A and S1B). To address whether FOXA2 expression represents an in vitro artifact following strong extrinsic activation of SHH signaling or whether FOXA2 expression occurs in the telencephalon during in vivo development, we performed histological analyses in the developing mouse and human forebrain. In mouse embryos (embryonic day 11.5 [E11.5]), FOXA2 expression within the mouse prosencephalon was segregated from the FOXG1 and NKX2.1 domains (Figure S1C). However, immunohistochemical analysis for FOXA2 in primary human forebrain tissue (CS15 embryo) confirmed expression in the telencephalic NKX2.1+ ganglionic eminence (Figures S1D–S1F). These in vivo data are in agreement with the in vitro hPSC differentiation data demonstrating (transient) FOXA2 expression during human ventral forebrain development.

Neuronal Differentiation and Migratory Properties of hESC-Derived NKX2.1+ Precursors

Cortical interneurons are important for balancing excitation and inhibition within cortical circuitry and play critical roles in controlling developmental plasticity. Cortical interneuron dysfunction has been implicated in various pathological conditions such as epilepsy, autism, and schizophrenia (Baraban et al., 2009; Insel, 2010; Lewis et al., 2005; Peñagarikano et al., 2011). Our data demonstrate that day 10–18 treated cells express cortical interneuron progenitor markers such as OLIG2, MASH1, and NKX6.2. At day 18 of differentiation, NKX2.1+ cells exhibit progenitor cell properties based on Nestin and Ki67 expression. Prolonged culture in the absence of extrinsic SHH activation led to a gradual decrease in Ki67 expression (Figures 3A–3C, upper panels) and increased percentages of cells expressing the neuronal precursor markers DCX and TUJ1 (Figures 3A–3C, lower panels). In addition, many GFP+ cells in the 10–18 and 2–18 conditions express γ-aminobutyric acid (GABA) and subsequently calbindin (Figures 3A–3C, lower panels), a marker of tangentially migrating cortical interneuron precursors (Anderson et al., 1997). Importantly, western blot analysis at day 32 showed that LHX6 protein, a marker of postmitotic, migratory cortical interneuron precursors in the mouse, was selectively enriched in the 10–18 condition. In contrast, the hypothalamic marker RAX was selectively enriched in the 2–18 condition (Figure 3D). Additional immunocytochemical data showed expression of DLX2 and ASCL1 in most neuronal progeny derived from the day 10–18 *NKX2.1::GFP*+ progenitors (Figures 3E–3G). These data indicate that following withdrawal of extrinsic SHH activators, *NKX2.1::GFP*+ progenitors give rise to region-specific postmitotic neurons including immature cortical interneurons.

We next asked whether hESC-derived putative cortical interneuron precursors (day 10–18 group) exhibit the characteristic migratory potential observed for primary cortical interneurons in the mouse (Anderson et al., 1997) and human (Letinic et al., 2002) brain. In both species, major subclasses of cortical interneurons undergo tangential migration on their way from the ventral telencephalon into the cortex (Anderson et al., 1997; Fertuzinhos et al., 2009; Letinic et al., 2002). *NKX2.1::GFP*+ cells at day 32 of differentiation were collected via FACS and injected into forebrain slices isolated from E13.5 mouse embryos. The cell injection was carefully targeted to the medial ganglionic eminence under microscopic visual guidance (Figure 3H). The migratory potential of *NKX2.1::GFP*+ cells and their ability to reach the cortex (see zone 2 in Figure 3H) were assessed for each treatment group (2–18, 6–18, and 10–18 of SHH treatment; Figures 3I–3L). At day 2 (Figure 3M), and more pronounced at day 6 after injection (Figure 3N), GFP+ cells were observed migrating from the injection site toward the cortex (zone 2). Remarkably, human cells from the 10–18 treatment, but not the two other treatment groups, showed a robust propensity for migration into the neocortical portions of the murine slice (Figures 3I–3N). These data suggest that day 10–18 treated cells exhibit migratory properties previously described for interneuron precursors derived from the primary mouse medial ganglionic eminence (MGE) (Sussel et al., 1999; Wichterle et al., 1999).

To further probe the migratory capacity of the day 2–18 versus 10–18 treated cells, we transplanted FACS-isolated *NKX2.1::GFP*+ cells into the neonatal neocortex of genetically immunocompromised mice. Four weeks after transplantation we observed extensive migration in both the radial and tangential planes within the mouse cortex, but only for the day 10–18 group (Figures 3O and 3P). Similar results were obtained upon transplantation into the adult cortex (Figure S2), though overall migration of *NKX2.1::GFP*+ cells by day 30 in vivo was less extensive compared to the neonatal grafts.

(F) Schematic illustration of the distinct time periods of SHH and purmorphamine treatment used in combination with the XLSB protocol. CTX, cortex; POA, preoptic area; HYPO, hypothalamus.

(G and H) Immunofluorescence for OLIG2 and FOXG1 in the *NKX2.1::GFP* line at day 18 of differentiation. Treatment with SHH after day 6 (6–18 and 10–18 groups) significantly increases the percentage of *NKX2.1::GFP*+ cells that coexpressed FOXG1, as quantified in (H). The scale bar in (G) represents 50 μm. Treatment with SHH after day 10 (10–18 group) enhanced the derivation of *NKX2.1::GFP*+ cells coexpressing OLIG2 (data are the mean ± SEM; *$p < 0.05$, ***$p < 0.001$, compared to 2–18 using ANOVA followed by Scheffe test). Expression of FOXG1, NKX2.1, and OLIG2 indicates a pattern characteristic of the ganglionic eminence (Tekki-Kessaris et al., 2001).

(I–K) Microarray data from cells sorted for NKX2.1::GFP expression at day 18 of differentiation, comparing gene-expression levels between the SHH day 10–18 protocol versus no SHH (I), the day 10–18 versus the day 2–18 protocol (J), and the day 10–18 versus day 6–18 protocol (K). Red bars indicate genes expressed at higher levels in the SHH 10–18 protocol; blue bars indicate genes expressed at lower levels in the day 10–18 protocol. All changes are significant at $p < 0.001$. See also Figure S1 and Table S1.

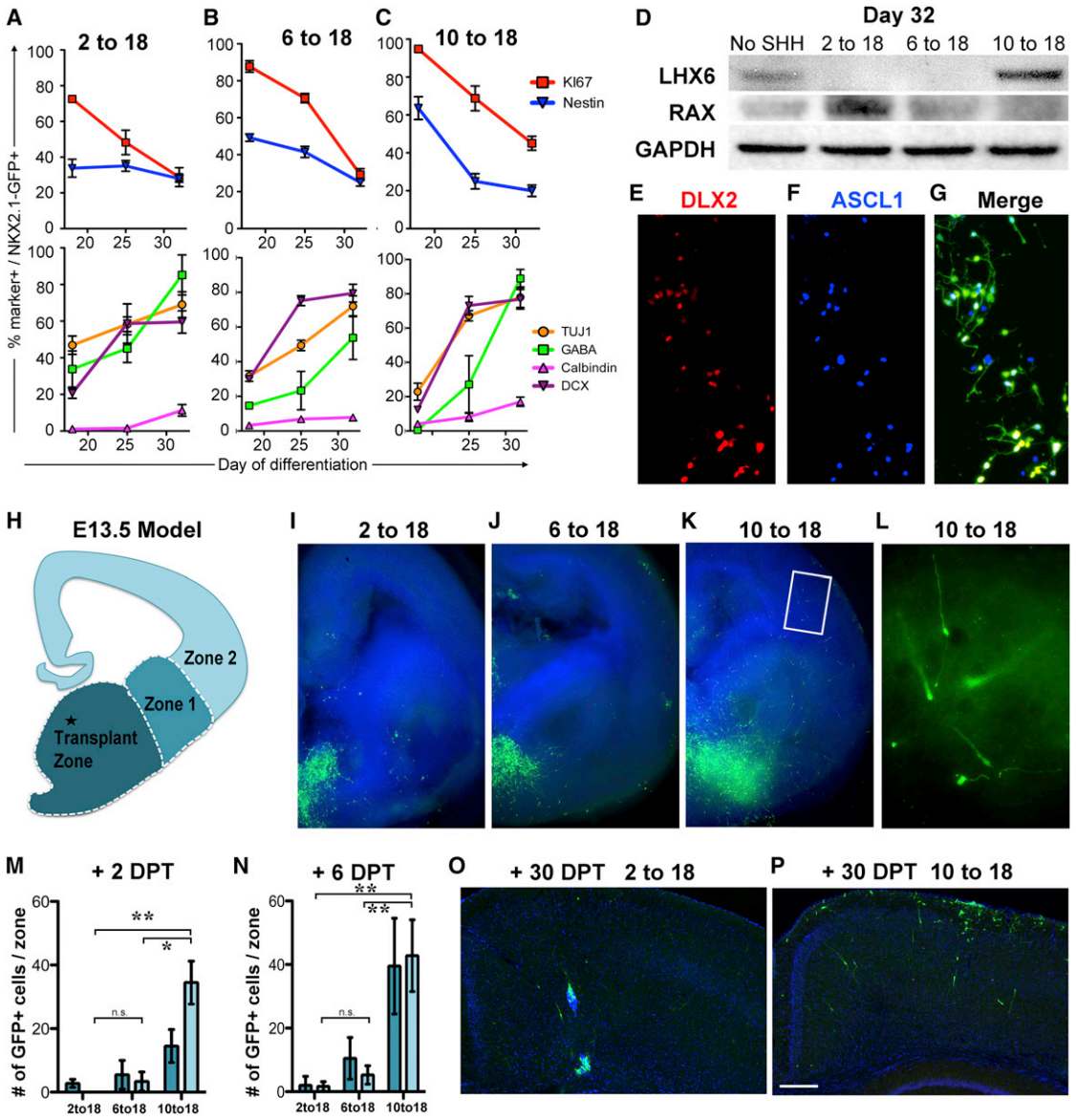

Figure 3. Conversion of Cycling Neural Progenitors to Neuronal Precursors and Assessment of Their Migratory Potential

(A–C) At day 18, cells from the three indicated protocols were subjected to FACS for *NKX2.1::GFP* expression, then replated and evaluated for colabeling with the markers indicated. For all three protocols there was a decline in colabeling with markers of progenitors (upper panels: red line, nestin; blue line, Ki67) and an increase in markers of neuronal differentiation (lower panels: green, GABA; yellow, TUJ1; purple, doublecortin [DCX]; pink, calbindin). Data are the mean ± SEM.

(D) Western blotting showed an increase in the hypothalamic-enriched protein RAX in the 2 to 18 condition and an increase in the MGE-enriched protein LHX6 in the 10 to 18 condition. Cells were sorted for NKX2.1::GFP prior to analysis.

(E–G) At day 32, many of the *NKX2.1::GFP*+ cells from the 10 to 18 condition also expressed DLX2 and ASCL1.

(H–N) Grafting of day 32-sorted *NKX2.1::GFP*+ cells into the MGE of E13.5 coronal mouse slice cultures. (H) Schematic of coronal hemisection demonstrating the site of transplantation and the zones for quantification of migration. (I and J) In both the 2 to 18 and the 6 to 18 conditions, very few cells migrated into zone 1, and fewer into zone 2. (K and L) Only the 10 to 18 condition demonstrated significant and robust migration into the cortical and striatal regions, with many GFP+ cells exhibiting bipolar morphologies consistent with a migratory cell (L). The regions where GFP+ cells were detected were quantified 2 (M) and 6 (N) days post transplantation (DPT). Data are the mean ± SEM; *$p < 0.05$, **$p < 0.01$ using ANOVA followed by Scheffe test.

(O and P) Transplantation of day 32-sorted *NKX2.1::GFP*+ cells (day 10 to 18 protocol) into the neocortex of neonatal mice followed by their evaluation in fixed sections at postnatal day 30. In marked contrast to the MGE-like cells from the SHH 10–18 protocol (P), neither the SHH 2–18 protocol (O) nor the SHH 6–18 protocol (data not shown) resulted in extensive migration from the graft site. The scale bar in (P) represents 200 μm.

See also Figures S2 and S3.

To determine the extent of interneuron precursor maturation in vivo, we assessed morphological appearance and the expression of interneuron-related markers in the grafted cells from the day 10–18 group (Figure S3). At 1–2 months after grafting into the neonatal cortex most human cells retained undifferentiated bipolar or unipolar morphologies and NKX2.1 expression.

Furthermore, essentially all grafted cells expressed the neuronal precursor marker DCX, including those with multipolar morphologies (Figure S3). As in rodents, the large majority of human interneuron precursors expressed GABA (46/51 GFP+ cells located at the section surface; Figure S3). In contrast, there was no colabeling for PV or SST, two proteins marking the major subclasses of Nkx2.1-lineage interneurons. These data suggest that even by 6 or 8 weeks posttransplant, the Nkx2.1::GFP+ cells had not yet differentiated into mature interneurons (Figure S3).

One explanation for the apparent lack of differentiation of the grafted GFP+ cells in the mouse host cortex could be that NKX2.1 is downregulated following maturation, as occurs in mouse cortical interneurons (Marin et al., 2000), resulting in the loss of GFP expression. For testing this possibility, sections were examined for expression of SC121, a human-specific panneuronal marker (Kelly et al., 2004). As expected, all GFP+ cells also expressed SC121 (Figure S3). At 6 weeks after transplantation, less than 10% of human cells were single positive for SC121 and lacked GFP expression (25 out of 372 SC121+ cells). In sum, perhaps due to the protracted rate of cortical interneuron maturation in vivo, transplantation studies did not result in mature cortical interneurons within the first 2 months of transplant.

Phenotypic and Synaptic Maturation of NKX2.1+ Neurons In Vitro

We have previously studied cortical interneuron development using a coculture system in which mouse embryonic MGE-derived progenitors are plated over a "feeder culture" composed mainly of mouse cortical pyramidal neurons and glia (Xu et al., 2004). To determine whether aspects of human interneuron maturation would be accelerated in this system relative to the xenografts, *NKX2.1::GFP*+ cells were collected via FACS at day 32 and replated onto cultures of dissociated embryonic mouse cortex (Figure 4A). The cortical cells were isolated from E13.5 mouse embryos, a stage prior to the immigration of the ventrally derived interneurons into the dorsal neocortex (Anderson et al., 1997). Thus, this coculture system mimics aspects of normal development with human NKX2.1+ cells developing in the presence of the glutamatergic cortical pyramidal neurons. Studies were performed in parallel using GFP+ cells derived from each of the three SHH treatment regimens (Figures 4B–4E). Roughly 80% of the GFP+ cells from the 10–18 treated "MGE-like" cultures, versus 40% from the 2–18 "hypothalamic-like" culture and 15% from the 6–18 culture, expressed GABA. Likewise, the 6–18 culture that is enriched for telencephalic (FOXG1+) cells but lacks expression of the interneuron precursor marker LHX6 (Figure 3D) was enriched for choline acetyltransferase (ChAT) neurons.

We next determined whether GFP+ cells from day 10–18 treated cultures (enriched for GABA neurons) undergo GABAergic synaptic transmission. Whole-cell patch-clamp electrophysiological studies (Figures 4F–4K) of identified GFP+ cells showed spontaneous firing in both day 10–18 and day 6–18 treated cultures (Figures 4H and 4I). However, only the day 10–18 group showed modulation of the firing rate of NKX2.1::GFP+ cells in response to the GABA type A (GABA-A) receptor antagonist bicuculline (Figure 4J). Because the cortical feeders contained very few murine interneurons (in both day 10–18 and day 6–18 coculture conditions), these results indicate that hPSC-derived GABAergic neurons mediate the inhibitory synaptic output. Accordingly, in the day 6–18 cultures in which GABAergic neurons are more rare (Figure 4C), the firing rates following bicuculline exposure remained unchanged (Figure 4K).

To further analyze synaptic inputs onto the *NKX2.1::GFP*+ cells from the day 10–18 protocol, we examined spontaneous postsynaptic currents and localization of inhibitory or excitatory synaptic markers. GFP+ cells cultured on the mouse cortical feeder for 30 days expressed high levels of vesicular GABA transporter (VGAT), present within the presynaptic terminal of GABAergic synapses. The subcellular localization of VGAT within GFP+ cells closely matched expression of the GABAergic postsynaptic marker gephyrin (Figures 5A–5E). Whole-cell patch-clamp analyses demonstrated that *NKX2.1::GFP*+ cells receive spontaneous inhibitory postsynaptic currents (sIPSCs; Figure 5F), which are reversibly blocked by the addition of the GABA-A receptor antagonist bicuculline. In addition, *NKX2.1::GFP*+ cells also receive excitatory inputs, as demonstrated by the presence of vesicular glutamate transporter 1 (VGLUT1) expression adjacent to GFP+ putative dendrites and colabeling with the postsynaptic excitatory synapse marker PSD-95 (Figure 5G–5K). Consistent with the presence of glutamatergic synaptic inputs, spontaneous excitatory postsynaptic currents (sEPSCs; Figure 5L) were also readily detected in the *NKX2.1::GFP*+ neurons. Additional analysis of spontaneous synaptic activity in *NKX2.1::GFP*+ cells is presented in Figure S4 and Table S2.

Cortical interneurons include a diverse set of neuron types with distinct roles in cortical development and function (Batista-Brito and Fishell, 2009). The relatively rapid pace of maturation in our mouse cortical feeder system allowed us to assess coexpression of more mature interneuron markers and to define neurotransmitter phenotypes beyond GABA and ChAT. In the day 2–18 group we observed a large percentage of GFP+ cells expressing tyrosine hydroxylase (TH) (Figure 6A), consistent with the dopaminergic nature of NKX2.1-lineage hypothalamic neurons (Yee et al., 2009). Immunohistochemistry showed high percentages of neuronal nitric oxide synthase (nNOS) cells in GFP+ cells from the day 2–18 and Calbindin in those from the day 10–18 group (Figures 6B and 6C). We also observed expression of markers characteristic of differentiated cortical interneurons, including SST and PV (Figures 6D and 6E), again mainly in the day 10–18 group. Representative images for each subgroup marker, coexpressed together with *NKX2.1::GFP*, are presented in Figures 6F–6J. No vasoactive intestinal polypeptide (VIP)- or calretinin-expressing neurons were observed, suggesting a lack of cells exhibiting features of the caudal ganglionic eminence (Xu et al., 2004). The derivation of NKX2.1+/PV+ neurons was particularly remarkable given the late developmental expression of this marker in cortical interneurons in vivo (Zecevic et al., 2011). Only a subset of the cells counted as GFP+/PV+ by the automated image analyses (Operetta high-content scanner, see Experimental Procedures) showed high levels of PV expression and exhibited interneuron-like morphologies (about 5% of total GFP+ cells, Figure 6J). Our results point to the need for further optimization of the derivation of selective cortical interneuron subtypes.

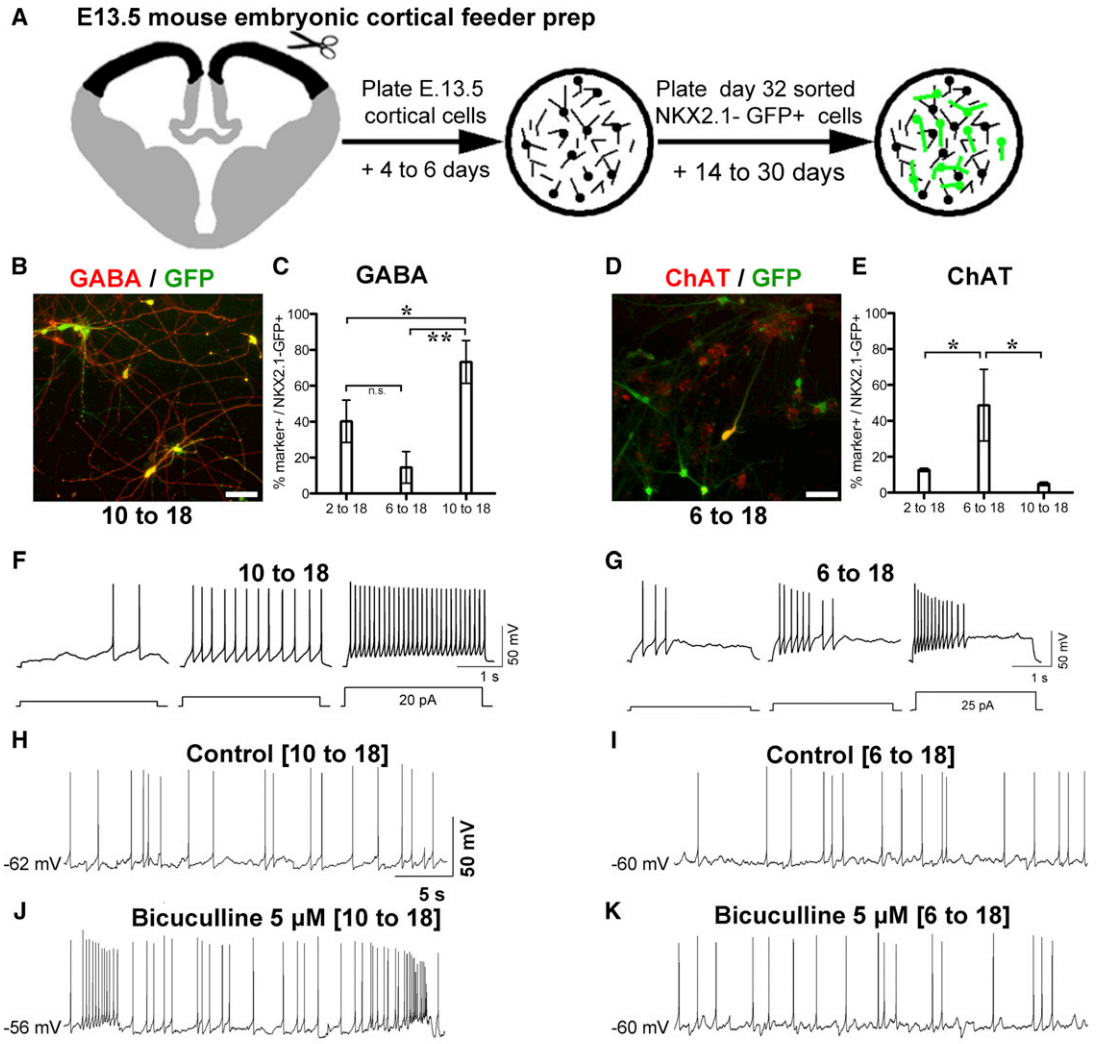

Figure 4. Maturation of NKX2.1+ Cells into Physiologically Active Neurons

(A) Preparation of cortical excitatory neuron cultures from E13.5 mice, onto which human *NKX2.1::GFP*+ cells (after FACS at day 32) are plated. The coculture system was critical for promoting neuronal maturation given the protracted in vivo maturation rates of NKX2.1+ cells.

(B–E) After 30 DIV, cultures from the SHH 10–18 conditions were enriched for *NKX2.1::GFP*+ cells that coexpress GABA (B), quantified in (C) (mean ± SEM; *p < 0.05, **p < 0.01 using ANOVA followed by Scheffe test). In contrast, only the SHH 6–18 condition was enriched for *NKX2.1::GFP* colabeling with ChAT (D), quantified in (E) (mean ± SEM; *p < 0.05 using ANOVA followed by Scheffe test).

(F and G) Spiking patterns of SHH day 10–18 (F) and SHH day 6–18 (G) neurons recorded at 28 DIV. Action potentials were initiated by protocols shown at the bottom.

(H–K) Spontaneous spiking was recorded from cultures enriched for GABAergic (SHH day 10 to 18) and cholinergic (6 to 18) neurons in the absence (H and I) and the presence (J and K) of the GABA-A receptor antagonist bicuculline. Bicuculline had little effect on the spontaneous firing activity in the 6 to 18 condition, consistent with the lack of GABAergic cells from either the mouse feeder or the human *NKX2.1::GFP*+ cells generated by this protocol.

The scale bars in (B) and (D) represent 50 µm.

However, the fact that PV+ hPSC-derived neurons could be generated at all suggests that the mouse cortical coculture strategy facilitates expression of cortical interneuron subtype markers.

Given the protracted maturation of *Nkx2.1::GFP*+, putative interneuron precursors in vivo, we were surprised to obtain morphological, marker-based, and physiological evidence of interneuron-like differentiation in the coculture system. We next tested whether similar results can be obtained by growing the same Nkx2.1::GFP+ cells on cultures enriched for human cortical projection neurons. The human cortical feeders were obtained upon differentiation of hESCs (modified XLSB conditions) followed by FACS for $CD44^{-}$/CD184+/CD24+ neurons (Yuan et al., 2011) (Figures S5A–S5D). The cortical identity of the hESC-derived neurons was confirmed by the expression of VGLUT1, MAP2, CTIP2, and SATB2. Only very few GFAP+ or Nestin+ cells were present under those conditions (Figures S5E–S5T).

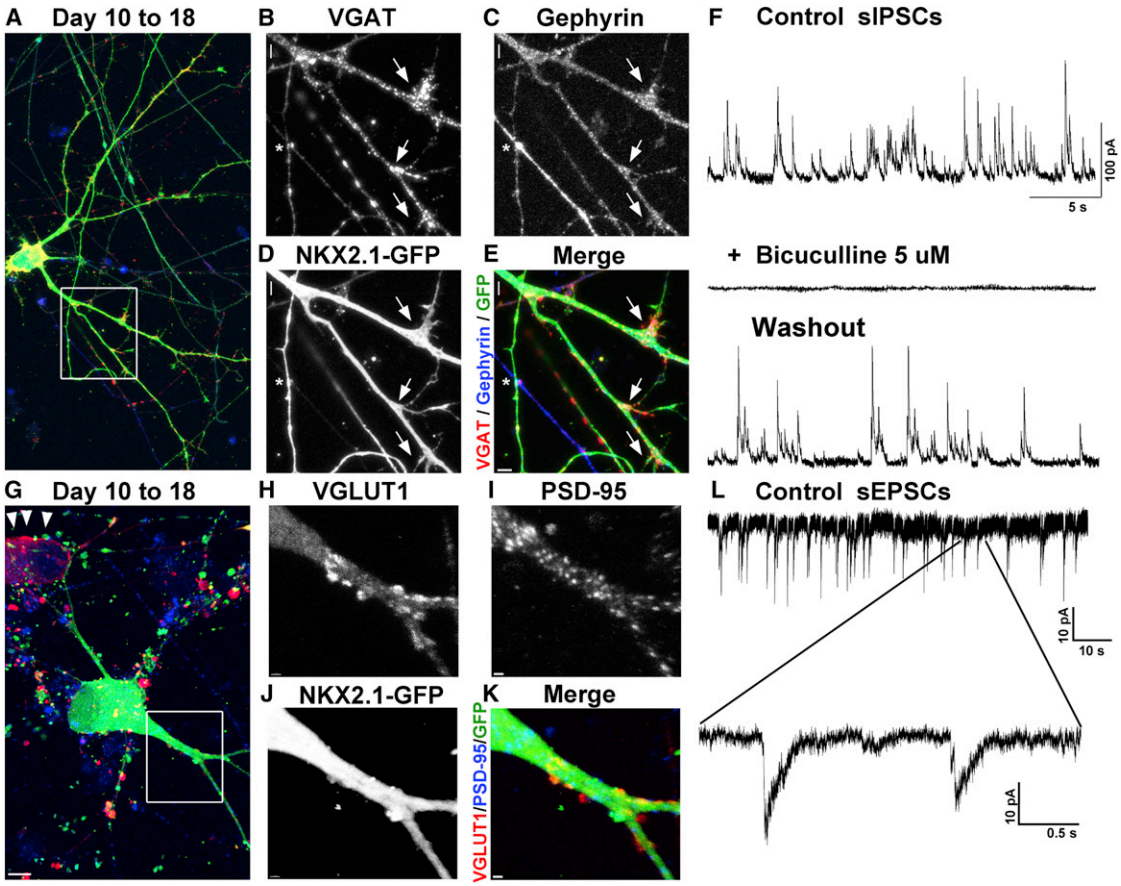

Figure 5. *NKX2.1::GFP*+ GABAergic Interneurons Receive Both Excitatory and Inhibitory Synaptic Inputs

(A–E) Collapsed z stack confocal image showing *NKX2.1::GFP*+, the vesicular GABA transporter (VGAT; red in A), and the postsynaptic GABAergic marker gephyrin (blue in A). The dendrites of this GFP+ cell that colabel with gephyrin are receiving VGAT-expressing presynaptic terminals (arrows). In addition, a GFP+ axonal process formed a VGAT+ presynaptic terminal adjacent to a GFP-negative, gephyrin-expressing postsynaptic process (asterisk).

(F) Whole-cell patch clamp reveals sIPSCs recorded from an *NKX2.1::GFP*+ neuron (SHH 10 to 18 protocol), which are reversibly blocked by the addition of the GABA-A receptor antagonist bicuculline.

(G–K) Collapsed z stack confocal image showing *NKX2.1::GFP*, VGLUT1 (red in G), and the postsynaptic marker PSD-95 (blue in C). This GFP+ cell has dendrites that colabel with PSD-95 and are adjacent to VGLUT1-expressing presynaptic terminals. Note the presence of a GFP-negative cell expressing VGLUT1 (red in G, arrowheads), confirming the presence of excitatory glutamatergic neurons in the culture. (L) Consistent with the apparent presence of glutamatergic synaptic inputs, sEPSCs were detected in the *NKX2.1::GFP*+ neurons (10 to 18). All cells were plated on mouse cortical feeder following FACS for *NKX2.1::GFP* at day 32. See also Figure S4.

Interestingly, we observed a consistent difference in electrophysiological maturation of NKX2.1+ cells plated on mouse versus human cortical feeders as shown in Table S2. Recordings were obtained at either 14–16 days in vitro (DIV) or 20–30 DIV for the mouse feeder condition and 20–30 DIV for the human cortical feeder condition. Analysis of the basic electrophysiological properties of both the 10– 18 and 6–18 groups plated on mouse feeders showed more mature characteristics at later time points of differentiation. There was significant hyperpolarization of the resting membrane potential (RMP) with time, as well as a decrease in the input resistance (Ri). In addition, the action potentials became faster and narrower, as evidenced by the decrease in the rise time and half-width. In contrast, GFP+ neurons from the day 10–18 condition that were recorded 20–30 days after plating on the human feeder layer retained relatively immature characteristics, comparable to the measurements seen in the younger 14–16 DIV neurons plated onto a mouse feeder layer. The RMP, action potential rise time, action potential half-width, and Ri were significantly different in the cortical feeder condition compared to the 10–18 neurons on mouse feeders recorded at the same DIV range. Sample traces depicting qualitative firing properties under the various conditions are shown in Figure S6.

These preliminary findings suggest that the pace of functional maturation is influenced by the local environment, though the corresponding mechanisms remain to be determined. Although it is possible that species-specific maturation rates trigger the timing of cortical interneuron maturation (e.g., by regulating activity), it is also possible that there are simply more astrocytes in mouse versus human feeders (Johnson et al., 2007). Future studies should include coculture with primary cortical neurons of human embryonic origin for further corroboration of our

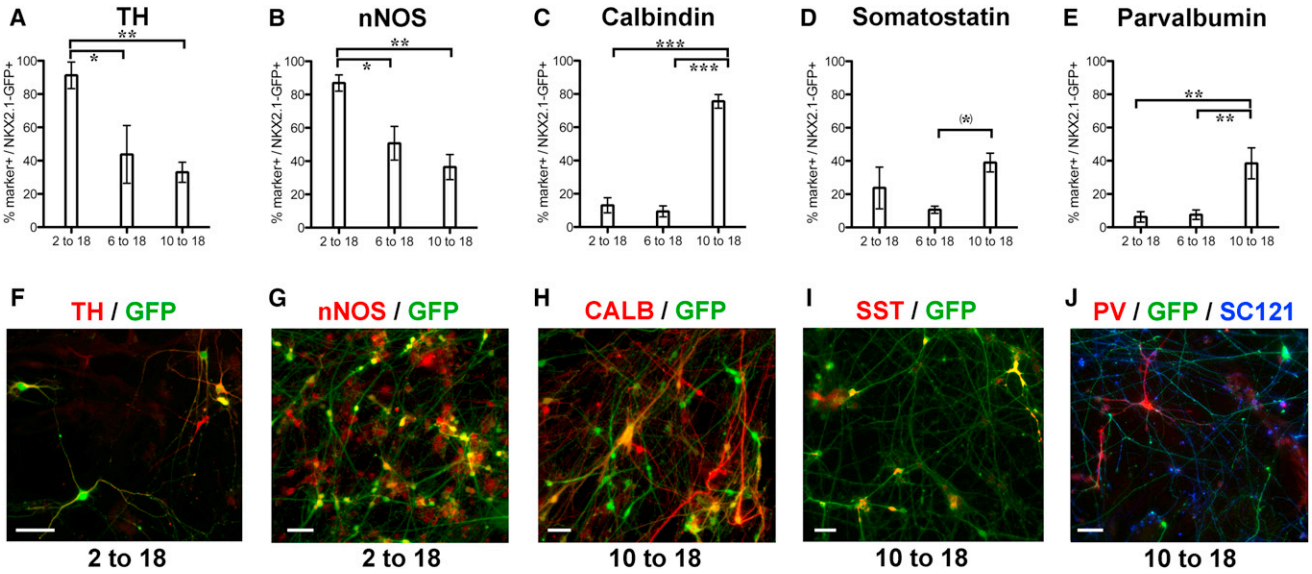

Figure 6. Neurochemical Profiling of *NKX2.1::GFP*+ Cells Grown on Mouse Cortical Feeders for 30 DIV

Cells were labeled by immunofluorescence for the markers indicated, and the results were quantified in graphs (A–E: mean ± SEM; *p < 0.05, **p < 0.01, ***p < 0.001 using ANOVA followed by Scheffe test: (*) p < 0.05 when compared directly to the 6–18 group; the p value did not reach significance in the standard Scheffe test: p = 0.08). Representative images of cellular labeling are shown in (F–J). In the SHH 2 to 18 condition, most of the cells colabeled with TH (A and F) and nNOS (B and G). In the 10 to 18 condition, many of the GFP+ cells colabeled with calbindin (Calb; C and H), somatostatin (SST; (D and I), and parvalbumin (PV; E and J), each of which is present in subpopulations of mature cortical interneurons in humans. All cells were plated on mouse cortical feeder following FACS for NKX2.1::GFP at day 32. The scale bars in (F)–(J) represent 50 μm. See also Figures S5 and S6 and Table S2.

findings. Independent of the mechanism, our data demonstrate that the mouse coculture conditions enhance maturation of hESC-derived cortical interneurons and enable functional in vitro studies.

DISCUSSION

The use of WNT-inhibitory molecules such as DKK1 has previously been proposed for the derivation of telencephalic and optic progenitors during mouse and human ESC differentiation (Lamba et al., 2006; Watanabe et al., 2005). We demonstrate that the tankyrase inhibitor XAV939 (Huang et al., 2009) can replace recombinant DKK1 for enhancing forebrain induction using the dual-SMAD inhibition protocol. The use of only three small molecules (XLSB protocol) renders our induction conditions well defined, cost effective, and robust across multiple cell lines. XLSB thus represents a general platform for generating forebrain lineages including cortical interneurons.

A recent paper demonstrated the importance of SHH dosage during in vitro ventral forebrain specification toward GSX2+, NKX2.1-negative progenitors capable of generating medium spiny striatal neurons (Ma et al., 2012). In addition to the SHH dose, timing can also affect the efficiency of ventral cell-fate specification (Fasano et al., 2010). A remarkable feature of the current study is that the difference in timing of SHH activation is sufficient for triggering the generation of distinct ventral progenitors of divergent anterior-posterior identity. We have previously reported the derivation of hESC-derived progenitors expressing markers of the hypothalamic anlage (Kriks et al., 2011) following early activation of SHH signaling in the presence of FGF8. Our day 2–18 data suggest that addition of FGF8 is not critical for directing hypothalamic progenitor fate. Cholinergic neuron derivation from *NKX2.1::GFP*+ progenitors of the 6–18 group should be of great value for modeling and treating disorders associated with loss of cognitive function. For example, in Alzheimer's disease basal forebrain cholinergic neurons are among the neurons most vulnerable during early stages of the disease (Whitehouse et al., 1982). However, the main focus of the current study is the derivation of human cortical interneuron lineages triggered in the day 10–18 protocol.

Our study points to several surprising differences in human versus mouse forebrain development, such as human-specific expression of FOXA2 in hESC-derived ventral forebrain progenitors and in CS15 human forebrain tissue. We speculate that transient FOXA2 expression reflects a prolonged requirement for SHH signaling during human development given the obvious differences in brain size and extended proliferation of SHH-dependent progenitors. To further address this hypothesis, it will be important to establish a time course of FOXA2 expression during human ventral forebrain development and to determine whether FOXA2 is linked to SHH expression as commonly observed in other FOXA2+ CNS domains such as the floor plate (Placzek and Briscoe, 2005).

Past studies have reported species differences in cortical interneuron development, based on the presence of ASCL1+ cells within the second-trimester human fetal cortex (Letinic et al., 2002). Those data led to the hypothesis that many, and perhaps most, human cortical interneurons are born within the cortex itself (Letinic et al., 2002). In contrast, studies in mice have demonstrated a subcortical origin of most, if not all, cortical

interneurons (Fogarty et al., 2007; Xu et al., 2004). Although our study was not specifically geared toward addressing this issue, we found restricted NKX2.1 expression within the ventral forebrain in CS15 human embryo and a complete lack of expression in the dorsal forebrain (see also the Allen Brain Atlas, http://human.brain-map.org/). Furthermore, the ability of hESC-derived cortical interneurons to migrate in our slice culture assay and in the developing murine cortex in vivo suggests that human cortical interneuron precursors have a capacity for tangential migration similar to that of their mouse counterparts. However, a distinctive feature in hESC-derived cortical interneurons was the persistent expression of NKX2.1. Nkx2.1 is extinguished in mouse cortical interneuron precursors by the time they leave the MGE prior to entering the cortex (Marin et al., 2000). Our in vitro data are consistent with findings in the human neocortex in vivo showing the presence of postmitotic NKX2.1+ neurons (Fertuzinhos et al., 2009). However, our data do not rule out the possibility that a subset of our human ESC-derived cells correspond to striatal interneurons, given that those share markers of cortical interneurons in the mouse while retaining NKX2.1 expression (Marin et al., 2000).

Current paradigms of modeling human psychiatric disease such as schizophrenia feature the use of patient-specific iPSC-derived neurons (Brennand et al., 2011; Marchetto et al., 2010; Paşca et al., 2011). However, those published studies were performed in mixed neural cultures of unclear neuronal subtype identity and with limited characterization of subtype-specific synaptic and functional properties. There is a convergence of postmortem findings that attempt to link genetic defects to psychiatric disorders, such as the interneuron-associated Erbb4 receptor in schizophrenia (Fazzari et al., 2010). Therefore, it is essential to have access to purified populations of mature cortical interneurons for modeling human disease. Our results demonstrate that the highly efficient derivation of cortical interneurons is possible following timed exposure to developmental cues.

We report that putative hESC-derived GABAergic interneurons receive synaptic inputs from both other human interneurons and from excitatory mouse projection neurons. In addition, cells with neurochemical properties of cortical interneurons adopt fairly mature physiological properties within 30 days of coculture. Future studies will be required to address the mechanisms of accelerated in vitro maturation of the *NKX2.1::GFP*+ neurons on mouse cortical cultures and to determine whether species-specific timing factors are involved, as suggested from our preliminary studies using hESC-derived cortical feeders. However, our data demonstrate that the proposed culture system can yield synaptically active cortical interneurons in vitro, a key prerequisite for modeling cortical interneuron pathologies in psychiatric disorders such as schizophrenia and autism. The generation of hESC-derived PV-expressing neurons and the presence of relatively rapid spiking, nonaccommodating neurons in these cultures is of particular interest given the implications of PV interneuron dysfunction in schizophrenia (Lewis et al., 2005). Fast-spiking PV+ cortical interneurons are observed late during primate prenatal development and continue their maturation into early adulthood (Anderson et al., 1995; Insel, 2010). Given the important role of PV+ neurons under various pathological conditions our data suggest that disease modeling of such states may be feasible using our differentiation strategies. Another key for the future will be the development of protocols that allow the enriched generation of specific cortical interneuron subgroups, such as sSST+ versus PV+ cells. Our previous results in MGE progenitors indicate that this decision may yet again be under the control of SHH signaling, with higher levels promoting SST+ and lower levels promoting PV+ neurons (Xu et al., 2010).

Finally, future studies will be required to address the full in vivo potential of human in vitro-derived cortical interneurons for applications in regenerative medicine. Our current study illustrates the remarkable migratory potential of the hESC-derived cortical interneurons upon transplantation into the neonatal mouse cortex. Transplantation studies into several adult CNS models of disease will be of particular interest given the potential use of cortical interneuron grafts in modulating pathological seizure activity (Baraban et al., 2009), treating aspects of Parkinson's disease (Martínez-Cerdeño et al., 2010), and inducing learning and plasticity within the postnatal brain (Southwell et al., 2010). One specific challenge for such transplantation studies is the protracted maturation of grafted hPSC-derived cortical interneuron precursors in vivo. Preliminary longer-term transplantation studies into the adult mouse cortex confirm their continued slow maturation rate, with NKX2.1+ putative interneuron precursors retaining immature growth cones and showing limited integration at 3 months post grafting (data not shown). Those data are in contrast to our in vitro coculture work, wherein rapid functional integration and phenotypic maturation was readily achieved. In sum, this study provides a framework for the generation of distinct ventral prosencephalic neuron types that can be used to study various aspects of development and serves as a powerful in vitro platform for studying the dysfunction of specific neuron types implicated in a myriad of neuropsychiatric diseases.

EXPERIMENTAL PROCEDURES

hESC Culture and Neural Differentiation

hESCs (WA-09, HES-3 (NKX2.1::GFP), and iPSCs (C72 and SeV6) were maintained on mouse embryonic fibroblasts and dissociated with accutase (Innovative Cell Technologies) for differentiation or dispase for passaging (Chambers et al., 2009). Differentiation media were described previously (Kriks et al., 2011): knockout serum replacer (KSR) and N2 medium for neural induction, and neurobasal medium + B27 (GIBCO) and N2 supplements (Invitrogen) for neuronal differentiation. Small-molecule compounds were as follows: XAV939 (2 μM; Stemgent;), LDN193189 (100 nM; Stemgent), SB431542 (10 μM; Tocris Bioscience), purmorphamine (1–2 μM; Calbiochem), ascorbic acid (200 μM), and dibutyryl-cyclic AMP (200 μM; both from Sigma-Aldrich). Recombinant growth factors were as follows: SHH (C25II; 50–500 ng/ml), Noggin (125 ng/ml), DKK1 (250 ng/ml), BDNF (10 ng/ml), all from R&D Systems, and FGF2 (5–10 ng/ml; Promega).

E13.5 Slice Migration Analysis

Coronal telencephalic slices (250 μm) were prepared as described previously (Anderson et al., 2001) and maintained in neurobasal medium/B27 with 5 ng/ml FGF2 (Promega). hESC-derived *NKX2.1::GFP*+ cells were isolated by FACS and carefully injected (~5,000 cells) into the periventricular region of the MGE using an oocyte microinjector (Nanoject II; Drummond Scientific). After 2–6 days, cultures were fixed and immunostained. For cell counting, zone 1 was defined as the region from the ventricular zone of the lateral ganglionic eminence extending to the pallial-subpallial border, and zone 2 was defined as the region from the lateral cortex through the neocortex to the cortical hem.

Mouse and Human Cortical Culture Preparation

The cortical feeder cultures were prepared by dissociating dorsal cortices from 250μm coronal slices of E13.5 mouse brain and cultured as described previously (Xu et al., 2010). For human cortical feeder preparation, cells were subjected to XLSB-mediated neural induction in the presence of cylcopamine and purified for CD24+/CD44$^-$/CD184+ at day 32 (see Supplemental Experimental Procedures for details).

Gene-Expression Profiling

Total RNA was isolated at day 18 of differentiation from FACS-sorted *NKX2.1::GFP*+ cells from three varying differentiation conditions and a "No SHH" condition that did not contain any GFP-expressing cells (Trizol, Sigma-Aldrich). Samples in triplicate for each group were processed for Illumina bead arrays (Illumina HT-12) by the Memorial Sloan-Kettering Cancer Center genomics core facility according to the specifications of the manufacturer.

Immunocytochemical Analyses

Cultures were fixed in 4% paraformaldehyde and processed for immunocytochemistry. Secondary antibodies were species-specific Alexa-dye conjugates (Invitrogen). The use of the primary antibodies is summarized in Table S3. For the automated quantification (Operetta, PerkinElmer), see Supplemental Experimental Procedures.

Transplantation Studies

Transplantation into the neonatal cortex of NOD-SCID IL2RG$^{-/-}$ mice was conducted as described previously (Wonders et al., 2008). In brief, ~50 × 10^3 cells were injected at following coordinates from bregma (2.0mm A, 2.5mm L, 1.0mm D), targeting cortical layers 3–6. All animal experiments were carried out in accordance with institutional and National Institutes of Health guidelines.

Human Tissue Analysis

Tissue derived from aborted human fetuses was obtained from the Department of Gynecology, University Bern, Switzerland. The study was approved by the ethics committee of the Medical Faculty of the University of Bern, Switzerland, and the ethics committee of the state of Bern, Switzerland (no. 52/91, 71/94, and 188/95). Written consent was given by the women seeking abortion.

Statistical Analysis

For all experiments, analysis was derived from at least three independent experiments. Statistical analysis was performed using ANOVA followed by a Scheffe test to for significance among individual groups (SYSTAT v.13).

FACS

All cells were dissociated using accutase (Stem Cell Technologies) for 30 min, then resuspended in neurobasal medium/B27 with Y27632 (10 μM; Tocris Bioscience) and sorted on a BD FACSAria II (gating for side scatter [SSC], forward scatter [FSC], and DAPI exclusion). For postsort analysis, data was processed using FlowJo (Tree Star) software.

Electrophysiology

Whole-cell voltage and current clamp recordings were performed as described previously (Ying et al., 2007). Details are provided in Supplemental Experimental Procedures.

ACCESSION NUMBERS

The raw data reported in this paper have been deposited in the GEO under accession number GSE46098.

SUPPLEMENTAL INFORMATION

Supplemental Information includes six figures, three tables, and Supplemental Experimental Procedures and can be found with this article online at http://dx.doi.org/10.1016/j.stem.2013.04.008.

ACKNOWLEDGMENTS

We would like to thank J. Hendrikx (Sloan-Kettering Institute [SKI] Flow Cytometry Core), A. Viale (SKI Genomics Core laboratory), M. Leversha (Molecular Cytogenetics Core), and E. Tu and M. Tomishima (SKI Stem Cell Facility) for excellent technical support. We further thank the Department of Gynecology (directors: M. Mueller and D. Surbek), University of Bern, Switzerland for providing us with the human fetal tissue. Studies using the *NKX2.1::GFP* hESC line were supported by grants from NYSTEM (S.A.), the European Commission project NeuroStemcell (L.S.), and the C.V. Starr Foundation (S.A. and L.S.). Experiments using hESC line WA-09 or iPSC lines were supported by NIMH grants 2RO1 MH066912 (S.A.) and 1RC1MH089690 (S.A. and L.S.) and by the Swiss National Science Foundation grant no. 31003A_135565 (H.R.W.).

Received: May 8, 2012
Revised: March 2, 2013
Accepted: April 12, 2013
Published: May 2, 2013

REFERENCES

Anderson, S.A., Classey, J.D., Condé, F., Lund, J.S., and Lewis, D.A. (1995). Synchronous development of pyramidal neuron dendritic spines and parvalbumin-immunoreactive chandelier neuron axon terminals in layer III of monkey prefrontal cortex. Neuroscience *67*, 7–22.

Anderson, S.A., Eisenstat, D.D., Shi, L., and Rubenstein, J.L. (1997). Interneuron migration from basal forebrain to neocortex: dependence on Dlx genes. Science *278*, 474–476.

Anderson, S.A., Marín, O., Horn, C., Jennings, K., and Rubenstein, J.L. (2001). Distinct cortical migrations from the medial and lateral ganglionic eminences. Development *128*, 353–363.

Baraban, S.C., Southwell, D.G., Estrada, R.C., Jones, D.L., Sebe, J.Y., Alfaro-Cervello, C., García-Verdugo, J.M., Rubenstein, J.L., and Alvarez-Buylla, A. (2009). Reduction of seizures by transplantation of cortical GABAergic interneuron precursors into Kv1.1 mutant mice. Proc. Natl. Acad. Sci. USA *106*, 15472–15477.

Batista-Brito, R., and Fishell, G. (2009). The developmental integration of cortical interneurons into a functional network. Curr. Top. Dev. Biol. *87*, 81–118.

Brennand, K.J., Simone, A., Jou, J., Gelboin-Burkhart, C., Tran, N., Sangar, S., Li, Y., Mu, Y., Chen, G., Yu, D., et al. (2011). Modelling schizophrenia using human induced pluripotent stem cells. Nature *473*, 221–225.

Chambers, S.M., Fasano, C.A., Papapetrou, E.P., Tomishima, M., Sadelain, M., and Studer, L. (2009). Highly efficient neural conversion of human ES and iPS cells by dual inhibition of SMAD signaling. Nat. Biotechnol. *27*, 275–280.

Dimos, J.T., Rodolfa, K.T., Niakan, K.K., Weisenthal, L.M., Mitsumoto, H., Chung, W., Croft, G.F., Saphier, G., Leibel, R., Goland, R., et al. (2008). Induced pluripotent stem cells generated from patients with ALS can be differentiated into motor neurons. Science *321*, 1218–1221.

Ebert, A.D., Yu, J., Rose, F.F., Jr., Mattis, V.B., Lorson, C.L., Thomson, J.A., and Svendsen, C.N. (2009). Induced pluripotent stem cells from a spinal muscular atrophy patient. Nature *457*, 277–280.

Eiraku, M., Watanabe, K., Matsuo-Takasaki, M., Kawada, M., Yonemura, S., Matsumura, M., Wataya, T., Nishiyama, A., Muguruma, K., and Sasai, Y. (2008). Self-organized formation of polarized cortical tissues from ESCs and its active manipulation by extrinsic signals. Cell Stem Cell *3*, 519–532.

Espuny-Camacho, I., Michelsen, K.A., Gall, D., Linaro, D., Hasche, A., Bonnefont, J., Bali, C., Orduz, D., Bilheu, A., Herpoel, A., et al. (2013). Pyramidal neurons derived from human pluripotent stem cells integrate efficiently into mouse brain circuits in vivo. Neuron *77*, 440–456.

Fasano, C.A., Chambers, S.M., Lee, G., Tomishima, M.J., and Studer, L. (2010). Efficient derivation of functional floor plate tissue from human embryonic stem cells. Cell Stem Cell *6*, 336–347.

Fazzari, P., Paternain, A.V., Valiente, M., Pla, R., Luján, R., Lloyd, K., Lerma, J., Marín, O., and Rico, B. (2010). Control of cortical GABA circuitry development by Nrg1 and ErbB4 signalling. Nature *464*, 1376–1380.

Fertuzinhos, S., Krsnik, Z., Kawasawa, Y.I., Rasin, M.R., Kwan, K.Y., Chen, J.G., Judas, M., Hayashi, M., and Sestan, N. (2009). Selective depletion of molecularly defined cortical interneurons in human holoprosencephaly with severe striatal hypoplasia. Cereb. Cortex *19*, 2196–2207.

Flames, N., Pla, R., Gelman, D.M., Rubenstein, J.L., Puelles, L., and Marín, O. (2007). Delineation of multiple subpallial progenitor domains by the combinatorial expression of transcriptional codes. J. Neurosci. *27*, 9682–9695.

Fogarty, M., Grist, M., Gelman, D., Marín, O., Pachnis, V., and Kessaris, N. (2007). Spatial genetic patterning of the embryonic neuroepithelium generates GABAergic interneuron diversity in the adult cortex. J. Neurosci. *27*, 10935–10946.

Gaspard, N., Bouschet, T., Hourez, R., Dimidschstein, J., Naeije, G., van den Ameele, J., Espuny-Camacho, I., Herpoel, A., Passante, L., Schiffmann, S.N., et al. (2008). An intrinsic mechanism of corticogenesis from embryonic stem cells. Nature *455*, 351–357.

Goulburn, A.L., Alden, D., Davis, R.P., Micallef, S.J., Ng, E.S., Yu, Q.C., Lim, S.M., Soh, C.L., Elliott, D.A., Hatzistavrou, T., et al. (2011). A targeted NKX2.1 human embryonic stem cell reporter line enables identification of human basal forebrain derivatives. Stem Cells *29*, 462–473.

Huang, S.M., Mishina, Y.M., Liu, S., Cheung, A., Stegmeier, F., Michaud, G.A., Charlat, O., Wiellette, E., Zhang, Y., Wiessner, S., et al. (2009). Tankyrase inhibition stabilizes axin and antagonizes Wnt signalling. Nature *461*, 614–620.

Insel, T.R. (2010). Rethinking schizophrenia. Nature *468*, 187–193.

Johnson, M.A., Weick, J.P., Pearce, R.A., and Zhang, S.C. (2007). Functional neural development from human embryonic stem cells: accelerated synaptic activity via astrocyte coculture. J. Neurosci. *27*, 3069–3077.

Kelly, S., Bliss, T.M., Shah, A.K., Sun, G.H., Ma, M., Foo, W.C., Masel, J., Yenari, M.A., Weissman, I.L., Uchida, N., et al. (2004). Transplanted human fetal neural stem cells survive, migrate, and differentiate in ischemic rat cerebral cortex. Proc. Natl. Acad. Sci. USA *101*, 11839–11844.

Kerwin, J., Yang, Y., Merchan, P., Sarma, S., Thompson, J., Wang, X., Sandoval, J., Puelles, L., Baldock, R., and Lindsay, S. (2010). The HUDSEN Atlas: a three-dimensional (3D) spatial framework for studying gene expression in the developing human brain. J. Anat. *217*, 289–299.

Kim, H., Lee, G., Ganat, Y., Papapetrou, E.P., Lipchina, I., Socci, N.D., Sadelain, M., and Studer, L. (2011). miR-371-3 expression predicts neural differentiation propensity in human pluripotent stem cells. Cell Stem Cell *8*, 695–706.

Kriks, S., Shim, J.W., Piao, J., Ganat, Y.M., Wakeman, D.R., Xie, Z., Carrillo-Reid, L., Auyeung, G., Antonacci, C., Buch, A., et al. (2011). Dopamine neurons derived from human ES cells efficiently engraft in animal models of Parkinson's disease. Nature *480*, 547–551.

Lamba, D.A., Karl, M.O., Ware, C.B., and Reh, T.A. (2006). Efficient generation of retinal progenitor cells from human embryonic stem cells. Proc. Natl. Acad. Sci. USA *103*, 12769–12774.

Letinic, K., Zoncu, R., and Rakic, P. (2002). Origin of GABAergic neurons in the human neocortex. Nature *417*, 645–649.

Lewis, D.A., Hashimoto, T., and Volk, D.W. (2005). Cortical inhibitory neurons and schizophrenia. Nat. Rev. Neurosci. *6*, 312–324.

Ma, L., Hu, B., Liu, Y., Vermilyea, S.C., Liu, H., Gao, L., Sun, Y., Zhang, X., and Zhang, S.C. (2012). Human embryonic stem cell-derived GABA neurons correct locomotion deficits in quinolinic acid-lesioned mice. Cell Stem Cell *10*, 455–464.

Marchetto, M.C., Carromeu, C., Acab, A., Yu, D., Yeo, G.W., Mu, Y., Chen, G., Gage, F.H., and Muotri, A.R. (2010). A model for neural development and treatment of Rett syndrome using human induced pluripotent stem cells. Cell *143*, 527–539.

Marin, O., Anderson, S.A., and Rubenstein, J.L. (2000). Origin and molecular specification of striatal interneurons. J. Neurosci. *20*, 6063–6076.

Maroof, A.M., Brown, K., Shi, S.H., Studer, L., and Anderson, S.A. (2010). Prospective isolation of cortical interneuron precursors from mouse embryonic stem cells. J. Neurosci. *30*, 4667–4675.

Martínez-Cerdeño, V., Noctor, S.C., Espinosa, A., Ariza, J., Parker, P., Orasji, S., Daadi, M.M., Bankiewicz, K., Alvarez-Buylla, A., and Kriegstein, A.R. (2010). Embryonic MGE precursor cells grafted into adult rat striatum integrate and ameliorate motor symptoms in 6-OHDA-lesioned rats. Cell Stem Cell *6*, 238–250.

Papapetrou, E.P., Tomishima, M.J., Chambers, S.M., Mica, Y., Reed, E., Menon, J., Tabar, V., Mo, Q., Studer, L., and Sadelain, M. (2009). Stoichiometric and temporal requirements of Oct4, Sox2, Klf4, and c-Myc expression for efficient human iPSC induction and differentiation. Proc. Natl. Acad. Sci. USA *106*, 12759–12764.

Paşca, S.P., Portmann, T., Voineagu, I., Yazawa, M., Shcheglovitov, A., Paşca, A.M., Cord, B., Palmer, T.D., Chikahisa, S., Nishino, S., et al. (2011). Using iPSC-derived neurons to uncover cellular phenotypes associated with Timothy syndrome. Nat. Med. *17*, 1657–1662.

Peñagarikano, O., Abrahams, B.S., Herman, E.I., Winden, K.D., Gdalyahu, A., Dong, H., Sonnenblick, L.I., Gruver, R., Almajano, J., Bragin, A., et al. (2011). Absence of CNTNAP2 leads to epilepsy, neuronal migration abnormalities, and core autism-related deficits. Cell *147*, 235–246.

Placzek, M., and Briscoe, J. (2005). The floor plate: multiple cells, multiple signals. Nat. Rev. Neurosci. *6*, 230–240.

Rakic, S., and Zecevic, N. (2003). Emerging complexity of layer I in human cerebral cortex. Cereb. Cortex *13*, 1072–1083.

Shi, Y., Kirwan, P., Smith, J., Robinson, H.P., and Livesey, F.J. (2012). Human cerebral cortex development from pluripotent stem cells to functional excitatory synapses. Nat. Neurosci. *15*, 477–486, S1.

Southwell, D.G., Froemke, R.C., Alvarez-Buylla, A., Stryker, M.P., and Gandhi, S.P. (2010). Cortical plasticity induced by inhibitory neuron transplantation. Science *327*, 1145–1148.

Sussel, L., Marin, O., Kimura, S., and Rubenstein, J.L. (1999). Loss of Nkx2.1 homeobox gene function results in a ventral to dorsal molecular respecification within the basal telencephalon: evidence for a transformation of the pallidum into the striatum. Development *126*, 3359–3370.

Tekki-Kessaris, N., Woodruff, R., Hall, A.C., Gaffield, W., Kimura, S., Stiles, C.D., Rowitch, D.H., and Richardson, W.D. (2001). Hedgehog-dependent oligodendrocyte lineage specification in the telencephalon. Development *128*, 2545–2554.

Watanabe, K., Kamiya, D., Nishiyama, A., Katayama, T., Nozaki, S., Kawasaki, H., Watanabe, Y., Mizuseki, K., and Sasai, Y. (2005). Directed differentiation of telencephalic precursors from embryonic stem cells. Nat. Neurosci. *8*, 288–296.

Whitehouse, P.J., Price, D.L., Struble, R.G., Clark, A.W., Coyle, J.T., and Delon, M.R. (1982). Alzheimer's disease and senile dementia: loss of neurons in the basal forebrain. Science *215*, 1237–1239.

Wichterle, H., Garcia-Verdugo, J.M., Herrera, D.G., and Alvarez-Buylla, A. (1999). Young neurons from medial ganglionic eminence disperse in adult and embryonic brain. Nat. Neurosci. *2*, 461–466.

Wonders, C.P., Taylor, L., Welagen, J., Mbata, I.C., Xiang, J.Z., and Anderson, S.A. (2008). A spatial bias for the origins of interneuron subgroups within the medial ganglionic eminence. Dev. Biol. *314*, 127–136.

Wu, H., Xu, J., Pang, Z.P., Ge, W., Kim, K.J., Blanchi, B., Chen, C., Südhof, T.C., and Sun, Y.E. (2007). Integrative genomic and functional analyses reveal neuronal subtype differentiation bias in human embryonic stem cell lines. Proc. Natl. Acad. Sci. USA *104*, 13821–13826.

Xu, Q., Cobos, I., De La Cruz, E., Rubenstein, J.L., and Anderson, S.A. (2004). Origins of cortical interneuron subtypes. J. Neurosci. *24*, 2612–2622.

Xu, Q., Guo, L., Moore, H., Waclaw, R.R., Campbell, K., and Anderson, S.A. (2010). Sonic hedgehog signaling confers ventral telencephalic progenitors with distinct cortical interneuron fates. Neuron *65*, 328–340.

Yee, C.L., Wang, Y., Anderson, S., Ekker, M., and Rubenstein, J.L. (2009). Arcuate nucleus expression of NKX2.1 and DLX and lineages expressing these transcription factors in neuropeptide Y(+), proopiomelanocortin(+), and tyrosine hydroxylase(+) neurons in neonatal and adult mice. J. Comp. Neurol. *517*, 37–50.

Ying, S.W., Jia, F., Abbas, S.Y., Hofmann, F., Ludwig, A., and Goldstein, P.A. (2007). Dendritic HCN2 channels constrain glutamate-driven excitability in reticular thalamic neurons. J. Neurosci. *27*, 8719–8732.

Yu, X., and Zecevic, N. (2011). Dorsal radial glial cells have the potential to generate cortical interneurons in human but not in mouse brain. J. Neurosci. *31*, 2413–2420.

Yuan, S.H., Martin, J., Elia, J., Flippin, J., Paramban, R.I., Hefferan, M.P., Vidal, J.G., Mu, Y., Killian, R.L., Israel, M.A., et al. (2011). Cell-surface marker signatures for the isolation of neural stem cells, glia and neurons derived from human pluripotent stem cells. PLoS ONE *6*, e17540.

Zecevic, N., Hu, F., and Jakovcevski, I. (2011). Interneurons in the developing human neocortex. Dev. Neurobiol. *71*, 18–33.